# Fatigue life under non-Gaussian random loading from various models

Alexis Banvillet, T. Lagoda, E. Macha, A. Nieslony, Thierry Palin-Luc, J-F. Vittori

# Fatigue life under non-Gaussian random loading from various models

A. Banvillet [a], T. Łagoda [b,*], E. Macha [b], A. Niesłony [b], T. Palin-Luc [a], J.-F. Vittori [c]

[a] *E.N.S.A.M. CER de Bordeaux, Laboratoire Matériaux Endommagement Fiabilité et Ingénierie des Procédés (EA 2727), Esplanade des Arts et Métiers, F-33405 Talence Cedex, France*

[b] *Technical University of Opole, Dept. Mechanics and Machine Design, ul. Mikołajczyka 5, 45-271 Opole, Poland*

[c] *Renault, Technocentre, Dir. Ingénierie des Matériaux, Sce 64130, API : TCR LAB 035, 1 Av. Golf, F-78288 Guyancourt Cedex, France*

**Abstract**

Fatigue test results on the 10HNAP steel under constant amplitude and random loading with non-Gaussian probability distribution function, zero mean value and wide-band frequency spectrum have been used to compare the life time estimation of the models proposed by Bannantine, Fatemi–Socie, Socie, Wang–Brown, Morel and Łagoda–Macha. Except the Morel proposal which accumulates damage step by step with a proper methodology, all the other models use a cycle counting method. The rainflow algorithm is used to extract cycles from random histories of damage parameters in time domain. In the last model, where a strain energy density parameter is employed, additionally spectral method is evaluated for fatigue life calculation in the frequency domain. The best and very similar results of fatigue life assessment have been obtained using the models proposed by Socie and by Łagoda–Macha, both in time and frequency domains for the last one.

*Keywords:* Fatigue life calculation; Strain energy; Spectral method; Rainflo algorithm; Random loading

## 1. Introduction

The known algorithms for assessment of fatigue life of machine components and structures under random loading can be divided into two groups. Some of them use numerical methods for cycle counting and damage accumulation step by step. On the other group, there are the so called 'spectral methods' based on the spectral analysis of stochastic processes. In the firs group, the loading of the material is usually represented by time courses of stresses and/or strains, and in the other group by their frequency characteristics, i.e. by the power spectral density function or its parameters. Lately [1–4], the strain energy density parameter has been proposed for fatigue life evaluation. This parameter seemed to be efficien in the case of fatigue life determination based on a cycle counting method [1,2,4]. The energy parameter includes the strain and stress histories and keeps the frequency character of the loading. Thus, we may ask if the strain energy density parameter can be applied in spectral methods where the power spectral density function plays the most important role.

The algorithms of fatigue life determination under multiaxial random loading must be also valid for the uniaxial random stress state. In a particular case, elements of machines and structures can remain in such a stress state for a certain life time. Verificatio of the model of multiaxial fatigue only for the uniaxial stress state includes one of the important stages of correctness these algorithms. This paper deals with the comparison of some selected models of fatigue life estimation under stationary non-Gaussian random axial loading on the basis of experimental data obtained for the 10HNAP steel in high cycle fatigue (HCF). In this paper the following models for multiaxial loading are analyzed and their predictions compared with experiments: Smith–Watson–Topper damage parameter used by Bannantine–Socie [5], Fatemi–Socie [5,6], Socie for HCF [7], Wang–Brown [8,9], Morel [10,11] and Łagoda–Macha [1–4].

* Corresponding author. Tel.: +48-77-4006-198; fax: +48-77-4006-343.

*E-mail address:* tlag@po.opole.pl (T. Łagoda).


doi:10.1016/j.ijfatigue.2003.08.017

**Nomenclature**

$A_W = W_a^{m'}N$ fatigue curve in an energy approach
a' for the energy approach, coeff cient allowing to include cycles with amplitudes below the fatigue limit from an arbitrary stress level
$A = \sigma_a^m N$ fatigue curve
$a$ coeff cient allowing to include stress amplitudes below the fatigue limit
$b$ tensile fatigue strength exponent
$b_0$ shear fatigue strength exponent
$c$ tensile ductility exponent
$c_0$ shear fatigue ductility exponent
$E$ Young modulus of the material
$M^+ = \sqrt{\frac{\lambda_4}{\lambda_2}}$ expected number of peaks in a time unit
$G$ shear modulus of the material
$G(f)$ power spectral density function
$m$ slope of the Wöhler curve,
$m' = m/2$ slope of the energy fatigue curve
$N_o$ number of cycles corresponding to the fatigue limit
$N_f$ number of cycles to failure
$n_i$ number of cycles with a stress amplitude $\sigma_{ai}$
$\vec{n}(\theta,\phi)$ unit normal vector to a material plane orientated by the angles $\theta$, $\varphi$ (spherical coordinates)
$p$, $q$, $r$ material parameters of the Morel approach
$P_{\vec{n}}$ material plane orientated by $\vec{n}(\theta,\phi)$
$q_1$ asymmetry or skewness
$q_2$ excess
$T_{Ba}$ life calculated according to the Bannantine–Socie model
$T_{Ch\text{-}D,W}$ life (in s) calculated according to the Chaudhury–Dover model with strain energy density parameter
$T_{exp}$ experimental fatigue life
$T_{FS}$ life calculated according to the Fatami–Socie model
$T_{Mo}$ life calculated according to the Morel model
$T_{RF,W}$ life calculated according to cycle counting algorithm from strain energy density parameter history
$T_{RMS}$ root mean square value of the macroscopic resolved shear stress
$T_{So}$ life calculated according to the Socie model
$T_{WB}$ life calculated according to the Wang–Brown model
$T_o$ observation time
$x$, $y$, $z$ axis linked with the specimen
$x'$, $y'$, $n$ arbitrary axis linked with the critical plane orientated by $\vec{n}(\theta,\phi)$
$W$ strain energy density parameter, distinguishing tension and compression,
$W_{af}$ fatigue limit according to the energy parameter
$\alpha = \frac{\lambda_2}{\sqrt{\lambda_0\lambda_4}}$ coeff cient of irregularity
$\epsilon'_f$ tensile fatigue ductility coeff cient
$\gamma = \sqrt{1-\alpha^2}$ coeff cient of the spectrum width
$\gamma'_f$ shear fatigue ductility coeff cient
$\Gamma(x)$ gamma function
$\nu$ Poisson's ratio
$\tau'_f$ shear fatigue strength coeff cient
$\sigma'_f$ axial fatigue strength coeff cient
$\theta,\phi$ angles orientating $\vec{n}$ in spherical coordinates system
$\mu_\sigma = \lambda_0$ variance of a stress history $\sigma(t)$
$\sigma_{a\ max}$ maximum amplitude in the history of stress after cycle counting by means of the rainf ow algorithm

$\sigma_{af}$ fatigue limit in fully reversed tension–compression

$\psi$ angle, from fixed axis in the plane $P_{\vec{n}}$, to define the direction where the resolved shear stress is computed

$\lambda_k = \int_0^\infty f^k G(f)\mathrm{d}f$ $k$th moment of one-sided power spectral density function of the stress history $\sigma(t)$

In the last model the strain energy density parameter is used both in time and frequency domain. In the first four models the damage parameter used has been originally proposed for cyclic loading, then used by some authors for variable amplitude multiaxial loading [5]. One aim of this paper is also to investigate if such models should be valid also for uniaxial random loading.

## 2. Comments about the methods using a cycle counting algorithm and based on the critical plane approach

With a general point of view, all the fatigue life calculation methods using a cycle counting algorithm can be summarized with the same methodology. First a cycle counting variable is chosen in order to extract the cycles (with their amplitude and mean value) from the variable amplitude or random multiaxial loading signal (stresses and/or strains). For the simulations presented hereafter the ASTM rainflow algorithm was used [13] (with 64 classes). All the random loadings are considered as stationary for life calculation. Secondly, a damage parameter Dp is chosen; it depends on stress-strain quantities. This damage parameter is computed on each material plane $P_{\vec{n}}$, orientated by the unit normal vector $\vec{n}(\theta,\phi)$ (Fig. 1), in order to look for the critical plane $P_{\vec{n}_c}$. Note that since the fatigue critical point is at the specimen surface the stress state is plane at this location, thus the number of planes to examine to look for the critical one can be reduced. All the computations were done by considering that $\theta = 45°$ and 90°, for $\phi$ varying between 0° and 180° as proposed in ref. [9,14]. Thirdly, to quantify the damage generated by each cycle identified with the counting algorithm it is necessary to use an equation relating the damage parameter and the number of cycles to failure $N_f$ under constant amplitude loading. It is then possible to compute the elementary damage caused by each extracted cycle and to accumulate step by step this damage by using, for instance, the linear Palmgren–Miner rule. Small cycles with a stress amplitude generating an elementary damage smaller than $10^{-12}$ were neglected in our computations. According to the S–N curve of the tested material, it corresponds to a stress amplitude smaller to 0.25 $\sigma_{af}$ in fully reversed tension. Finally, the fatigue life is calculated by assuming a threshold value of the total damage sum. One is usually used for this threshold value as it was done in this paper, but some authors have shown that this limit can vary in a large interval [15,16].

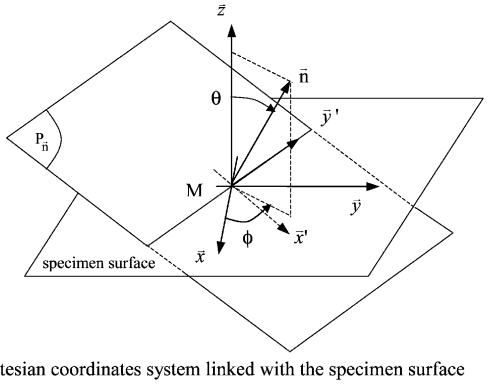


$(\vec{x},\vec{y},\vec{z})$ cartesian coordinates system linked with the specimen surface

$(\vec{x}',\vec{y}',\vec{n})$ cartesian coordinates system linked with the plane $P_{\vec{n}}$ orientated by $\vec{n}$.

Fig. 1. Coordinates system used to define the unit normal vector $\vec{\mathbf{n}}$ orientating each material plane $P_{\vec{\mathbf{n}}}$ at the point M on the surface of the specimen.

## 3. Fatemi and Socie's model

According to Fatemi and Socie (FS) [5–7], for each material plane $P_{\vec{n}}$, the cycle counting method has to be applied on two variables: the shear strains $\gamma_{nx'}(t)$ and $\gamma_{ny'}(t)$. The critical plane is, for each of these two counting variables, the plane experiencing the highest shear strain range. For the materials where the fatigue crack initiation is dominated by plastic shear strains FS recommend to use the following damage parameter: $Dp_{FS} = \gamma_a(1 + k_1\sigma_{n,max}/\sigma_y)$ related to the Manson–Coffin curve in torsion by equation:

$$\gamma_a(1 + k_1\sigma_{n,max}/\sigma_y) = \frac{\tau'_f}{G}(2N_f)^{b_0} + \gamma'_f(2N_f)^{c_0}. \quad (1)$$

The term on the left-hand side represents the damage parameter on the critical plane. For each loading cycle extracted by the rainflow method, $\gamma_a$ is the shear strain amplitude ($\Delta\gamma_{nx'}/2$ or $\Delta\gamma_{ny'}/2$). $\sigma_{n,max}$ is the maximum of the normal stress on the critical plane, during the current cycle of the counting variable $\gamma_{nx'}(t)$ or $\gamma_{ny'}(t)$ (Fig. 2). $\sigma_y$ is the yield stress of the material in tension. In this damage parameter, $k_1$ is a material constant identified by fitting uniaxial against pure torsion fatigue data.

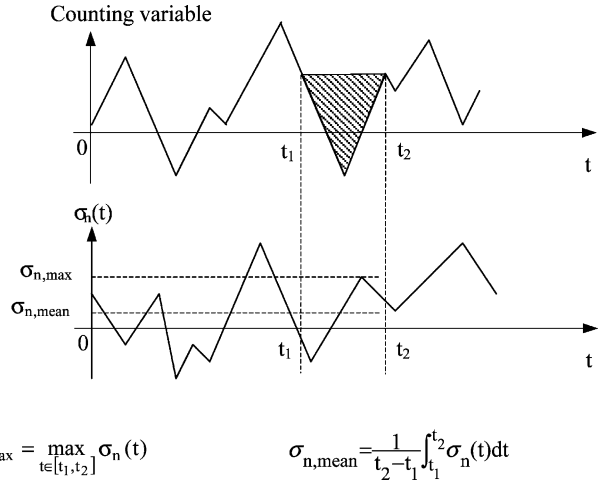


$$\sigma_{n,max} = \max_{t\in[t_1,t_2]} \sigma_n(t) \qquad \sigma_{n,mean} = \frac{1}{t_2 - t_1}\int_{t_1}^{t_2} \sigma_n(t)dt$$

Fig. 2. Definition of the mean and maximum normal stress during an extracted cycle (from $t_1$ to $t_2$) with the rainflow algorithm.

The right-hand side of Eq. (1) is the description of the strain-life Manson–Coffin curve in torsion. When the strain-life Manson–Coffin torsion curve is not known, FS propose to approximate this curve from the tensile strain-life curve [6]. The algorithm used to apply this fatigue life calculation method is detailed in a flow chart in Appendix 1.

## 4. Smith–Watson–Topper parameter used by Bannantine and Socie

For the materials where short fatigue cracks grow on the plane perpendicular to the maximum principal stress and strain (mode I), Bannantine and Socie [5] recommend using the Smith–Watson–Topper (SWT) damage parameter: $Dp_{SWT} = \varepsilon_{n,a}\sigma_{n,max}$. For each material plane $P_{\vec{n}}$, the cycle counting method is applied on the normal strain $\varepsilon_n(t)$. The relation between the damage parameter and the number of cycles to failure $N_f$ for a constant amplitude loading in tension is:

$$\varepsilon_{n,a}\sigma_{n,max} = \frac{\sigma'^2_f}{E}(2N_f)^{2b} + \sigma'_f\varepsilon'_f(2N_f)^{b+c} \quad (2)$$

In this equation and for each load cycles extracted by the rainflow method, $\varepsilon_{n,a}$ is the amplitude of the normal strain and $\sigma_{n,max}$ is the maximum normal stress during the current cycle of the counting variable $\varepsilon_n(t)$ (Fig. 2). The algorithm used to compute life according to this model is shown in Appendix 2.

## 5. Socie's proposal for HCF regime

According to Fatemi and Socie for HCF and ductile materials most of the fatigue life is consummed by crack nucleation on the planes where the shear stress is maximum. In this case Socie [7] proposes the following stress based approach by using as damage parameter: $Dp_{So} = \tau_a + k_2\sigma_{n,max}$. This is the linear combination of the shear stress amplitude $\tau_a$ and the maximum normal stress $\sigma_{n,max}$, acting on the critical plane, both during the load cycle (Fig. 2). For each material plane $P_{\vec{n}}$, the cycle counting algorithm has to be applied on two counting variables: the shear stresses $\tau_{nx'}(t)$ and $\tau_{ny'}(t)$. The critical plane is, the plane experiencing the highest shear stress range ($\Delta\tau_{nx'}(t)$ or $\Delta\tau_{ny'}(t)$). The relation linking the damage parameter and the number of cycles to failure under constant amplitude loading is given by the following equation:

$$\tau_a + k_2\sigma_{n,max} = \tau'_f(2N_f)^{b_0}. \quad (3)$$

The right-hand side of this equation is the elastic part of the strain-life curve. $k_2$ is a material parameter identified by fitting tension and torsion fatigue data. The algorithm used to apply this method is illustrated in Appendix 3.

## 6. Wang and Brown's model

Wang and Brown [8,9] developed a model first restricted to low cycle fatigue (LCF) and medium cycle fatigue (MCF) according to the assumption that fatigue crack growth is controlled by the maximum shear strain. For each material plane $P_{\vec{n}}$, the rainflow cycle counting method has to be applied on two counting variables: the shear strains $\gamma_{nx'}(t)$ and $\gamma_{ny'}(t)$. The critical plane is the plane experiencing the highest shear strain range. Assuming that, during one cycle the normal strain excursion $\Delta\varepsilon_n$ plays an important additional role, Wang and Brown propose the following expression as damage parameter: $Dp_{WB} = \gamma_a + S\,\Delta\varepsilon_n$, where $\gamma_a$ is the shear strain amplitude and $S$ is a material parameter identified by fitting tension against torsion fatigue data. The relation between the damage parameter and the life time is expressed as

$$\gamma_a + S\,\Delta\varepsilon_n = (1 + \nu_e + S(1-\nu_e))\frac{\sigma'_f - 2\sigma_{n,mean}}{E}(2N_f)^b + (1 + \nu_p + S(1-\nu_p))\ \varepsilon'_f(2N_f)^c \quad (4)$$

where $\nu_e$ and $\nu_p$ are respectively the elastic and plastic Poisson's ratio of the material. $\sigma_{n,mean}$ is the mean normal stress on the critical plane during each extracted cycle (Fig. 2) of counting variable $\gamma_{nx'}(t)$ or $\gamma_{ny'}(t)$.

The algorithm used to compute the fatigue life according to the Wang–Brown model is shown in Appendix 4.

## 7. Morel's approach

Morel developed a model for polycrystalline metals in HCF based on the mesoscopic plastic strain accumu-

lation [10,11,12]. This author assumes that the mechanical behaviour of each grain of the material follows a three phase law: hardening, saturation and softening. The mesoscopic plastic strain $\Gamma$ is chosen as a damage parameter. By assuming that each crystal of the material obeys to a combined isotropic and kinematic hardening rule when flowing plastically, the initiation of slip in each grain is described by the Schmid criterion. According to Morel a fatigue crack initiates if the cumulated mesoscopic plastic strain reaches a critical value $\Gamma_f$ depending on the material. For multiaxial constant amplitude loading Morel uses the high cycle multiaxial fatigue criterion proposed by Papadopoulos, who demonstrated that the limit value of the $T_\sigma$ parameter (which is an upper bound value of the plastic mesostrain accumulated in some crystals of an elementary volume $V$) is depending on the maximum value of the hydrostatic stress $\Sigma_{H,max}$ during a loading cycle

$$\max_{\theta,\varphi} T_\sigma(\theta,\varphi) \quad + \quad \alpha\Sigma_{H,max} \leq \beta \tag{5}$$

In this approach the critical plane, orientated by the unit normal vector defined by the angles $(\theta,\varphi)$, is the plane experiencing the maximum value, noted $T_\Sigma$, of $T_\sigma(\theta,\varphi)$. From this criterion, Morel defines a limit multiaxial loading (so that $T_{\Sigma lim} + \alpha\Sigma_{H,max,lim} = \beta$) depending on both the amplitude $\Sigma_{H,a}$ and the mean value $\Sigma_{H,m}$ of the hydrostatic stress

$$T_{\Sigma lim} = \frac{-\alpha\Sigma_{H,m} + \beta T_\Sigma}{\alpha + \dfrac{T_\Sigma}{\Sigma_{H,a}}} \cdot \frac{T_\Sigma}{\Sigma_{H,a}} \tag{6}$$

Then from the macroscopic shear stress amplitude $C_A$ acting on the critical plane, the limit value $\tau_{lim}$ of the mesoscopic shear stress during the saturation phase is equal to the ratio $T_{\Sigma lim}/H$ where H is a 'phase-difference parameter': $H = T_\Sigma/C_A$. Finally, from the hypothesis that a fatigue crack initiates on the critical plane in the most stressed grains, Morel proposed the following S–N curve equation, for constant amplitude loadings

$$N_f = p \ln\left(\frac{C_A}{C_A - \tau_{lim}}\right) + q\left(\frac{\tau_{lim}}{C_A - \tau_{lim}}\right) - \frac{r}{C_A} \tag{7}$$

where $p$, $q$ and $r$ are three material parameters (function of the hardening, saturation and softening phases of the crystal) which can be identified from only one experimental S–N curve.

Under variable amplitude loading, the amplitude, mean value and phase difference of each stress $\Sigma_{ij}(t)$ cannot be defined. In this case, to simplify the fatigue life prediction problem Morel proposed to consider as critical plane, the most damaging one. One way to localize this plane is to look for the maximum value of $T_{\sigma,RMS}(\theta,\phi)$ (noted $T_{\Sigma,RMS}$), which is the root mean square of the macroscopic resolved shear stress acting on a line orientated by the unit vector $\vec{m}(\psi)$. This unit vector is determined by the angle $\psi$ from fixed axis in the plane defined by its angles $\theta$ and $\phi$ (spherical coordinates) [10,11].

$$T_{\Sigma,RMS} = \max_{\theta,\phi} T_{\sigma,RMS}(\theta,\phi) \text{ with } T_{\sigma,RMS}(\theta,\phi) = \sqrt{\int_{\psi=0}^{2\pi} T_{RMS}^2(\theta,\phi,\psi)\,d\psi} \tag{8}$$

Once the critical plane located, the 'phase parameter' $H$ is computed with equation

$$H = \frac{T_{\Sigma RMS}}{C_{RMS}} \text{ where } C_{RMS} = \max_{\psi} T_{RMS}(\psi) \tag{9}$$

on this plane (Appendix 5).

After this step, the time history of the hydrostatic stress $\Sigma_H(t)$ and of the resolved shear stress $\tau(\psi,t)$on the critical plane is computed. The amplitude of the hydrostatic stress and its mean value between two extreme at $t_i$ and $t_{i+1}$ of the macroscopic resolved shear are respectively: $\Sigma_{H,a} = |\Sigma_H(t_{i+1}) - \Sigma_H(t_i)|/2$ and $\Sigma_{H,m} = (\Sigma_H(t_i) + \Sigma_H(t_{i+1}))/2$. The amplitude of the resolved shear stress is $\tau_a(\psi) = |\tau_a(\psi,t_{i+1}) - \tau_a(\psi,t_i)|/2$. By assuming that $T_\Sigma/\tau_a(\psi)$ (for each transition $t_i$ to $t_{i+1}$) and $H = T_{\Sigma RMS}/C_{RMS}$ (for all the load sequence) are the same; $T_\Sigma$ is computed for the current transition by: $T_\Sigma = H\,\tau_a(\psi)$. Thus, for each transition, the application of Eq. (6) allows us to estimate the limit value of the mesoscopic shear stress with $\tau_{lim} = \dfrac{T_{\Sigma_{lim}}}{T_{\Sigma RMS}/C_{RMS}}$ for the direction $\vec{m}(\psi)$. Finally, the saturation yield limit of the crystal, in this direction of the critical plane, can be estimated from the mean value $(\tau_{lim})_{mean}$ (calculated over the whole sequence) of the saturation shear stress at each loading transition. This calculation is done over each direction of the critical plane; the number of sequences to fatigue crack initiation is deduced from the direction leading to the highest accumulated damage. Note that for the Morel method the damage accumulation is done step by step without any cycle counting method (rainflow for instance) according to the rules described in the following paragraph. Thus, the calculated life is sensitive to the order of the stress levels.

To apply this calculation method the parameters $p = \dfrac{c+\mu}{4}(1/g + 1/h)$, $q$, $r = q\,\dfrac{\tau_y^{(0)}}{g}$ of the S–N curve (7) are necessary but the initial yield stress of the crystal $\tau_y^{(0)}$ is also needed to be able to cumulate damage. The identification of these four parameters requires a specific damage cumulative fatigue test (detailed in [11]) to identify separately the hardening parameter $g$. Damage is cumulated according to the following rules. During the hardening phase $\dot{\tau}_y = \dfrac{1}{\dfrac{c+\mu}{g} + 1}\sqrt{\underline{\dot{\tau}}\cdot\underline{\dot{\tau}}}$, and during the softening

phase $\dot{\tau}_y = \dfrac{1}{1 - \dfrac{c+\mu}{h}}\sqrt{\dot{\underline{\tau}}\cdot\dot{\underline{\tau}}}$. If the yield stress of the crystal $\tau_y$ is equal to $\tau_{\lim}$ the saturation phase is reached. Then, the softening phase begins as soon as $\Omega = 4q\tau_{\lim}$ where $\dot{\Omega} = \sqrt{\dot{\underline{\tau}}\cdot\dot{\underline{\tau}}}$. Fatigue crack initiates in the grain when the crystal yield stress reaches zero.

## 8. The strain energy density parameter

A change of strain energy density, applied in theory of plasticity, has been proposed as a parameter to describe multiaxial fatigue [1–4]. In order to distinguish the work under tension and compression during a uniaxial fatigue cycle, Łagoda and Macha introduce the functions sgn[$\sigma(t)$] and sgn[$\varepsilon(t)$] as follows,

$$W(t) = \frac{1}{2}\sigma(t)\varepsilon(t)\frac{\mathrm{sgn}[\sigma(t)] + \mathrm{sgn}[\varepsilon(t)]}{2} \tag{10}$$

where

$$\mathrm{sgn}[x] = \begin{cases} +1 & \text{for } x > 0 \\ 0 & \text{for } x = 0 \\ -1 & \text{for } x < 0 \end{cases},$$

$\sigma(t)$, $\varepsilon(t)$ are stress and strain time history in the critical plane. For uniaxial loading it means $\sigma(t) = \sigma_x(t)$ and $\varepsilon(t) = \varepsilon_x(t)$.

Eq. (10) expresses positive and negative values of the strain energy density parameter in a fatigue cycle and it allows to distinguish energies under tension and compression. If this parameter is positive, the material is subjected to tension. When it is negative, the material is subjected to compression. Eq. (10) has another advantage: energy course in time has the zero mean value when cyclic stresses and strains change symmetrically in relation to the zero levels.

If the cyclic stresses and strains reach their maximum values $\sigma_a$ and $\epsilon_a$, the maximum value of the energy parameter (10) and its amplitude are the same: $W_a = W_{\max}$.

$$W_a = \frac{1}{2}\sigma_a\varepsilon_a \tag{11}$$

Assuming $W(t)$ according to Eq. (10) as a fatigue failure parameter, the standard characteristic curves of cyclic fatigue ($\sigma_a - N_f$) and($\varepsilon_a - N_f$) can be rescaled to obtain a new curve, ($W_a - N_f$). In the case of high-cycle fatigue, when the characteristic ($\sigma_a - N_f$) is used, the $\sigma_a$ axis should be replaced by $W_a$, where

$$W_a = \frac{\sigma_a^2}{2E}. \tag{12}$$

So we obtain,

$$W_a = \frac{(\sigma'_f)^2}{2E}(2N_f)^{2b} = \frac{(\sigma'_f)^2}{2E}(2N_f)^{b'} \tag{13}$$

From among the cyclic counting methods, the rainf ow algorithm and the Palmgren–Miner hypothesis of damage accumulation have been chosen [1,2,4]. The life time, $T_{RF}$ is calculated from cycles and half-cycles in the time observation $T_o$ of stress history $\sigma(t)$,

$$T_{RF} = \frac{T_o}{\sum_{i=1}^{k}[n_i/(N_o(\sigma_{af}/\sigma_{ai})^m)]} \text{ for } \sigma_{ai} \geq a\ \sigma_{af}, a = 0.5 \tag{14}$$

For spectral method the Chaudhury–Dover model [17] for wide-band frequency processes has been chosen [17–20]

$$T_{Ch\text{-}D} = \frac{A}{M^+(2\mu_\sigma)^{\frac{m}{2}}\left[\dfrac{\gamma^{m+2}}{2\sqrt{\pi}}\Gamma\left(\dfrac{m+1}{2}\right) + \dfrac{3\alpha}{4}\Gamma\left(\dfrac{m+2}{2}\right)\right]}. \tag{15}$$

The models—Eqs. (11) and (12) in energy notation with parameter $W(t)$—Eq. (10)—can be modif ed as follows:

$$T_{RF,W} = \frac{T_o}{\sum_{i=1}^{k}[n_i/(N_o(W_{af}/W_{ai})^{m'})]} \tag{16}$$

for $W_{ai} \geq a' W_{af}$, $a' = 0.25$

$$T_{Ch\text{-}D,W} = \frac{A_W}{M^+(2\mu_W)^{\frac{m'}{2}}\left[\dfrac{\gamma^{m'+2}}{2\sqrt{\pi}}\Gamma\left(\dfrac{m'+1}{2}\right) + \dfrac{3\alpha}{4}\Gamma\left(\dfrac{m'+2}{2}\right)\right]} \tag{17}$$

where $M^+, \mu_W, \gamma, \alpha$ are as in Eq. (15), remember that these parameters are determined from the power spectral density function, $G_W(f)$ of the energy parameter $W(t)$ (see def nition in Appendix 6).

A block diagram of calculation algorithms is shown in Appendix 6. Let us remember that calculations according to the cycle counting method are done in a time domain and calculations using the spectral method—by estimation of the power spectral density function—are done in the frequency domain.

## 9. Fatigue test conditions and results

Flat smooth specimens were cut out from 10HNAP steel ($R_e$ = 389 MPa, $R_m$ = 566 MPa, $A_{10}$ = 31%, $Z$ = 29.1%, $E$ = 215 GPa, $\nu$ = 0.29). From constant amplitude fatigue tests on smooth specimens in fully reversed ten-

Table 1
The fatigue test data of 10HNAP steel under random loading and the calculation of results of life time according to various models

| No. | $\sigma_{amax}$ (MPa) | $\sigma_{RMS}$ (MPa) | $T_{exp}$ | $T_{FS}$ (s) | $T_{Ba}$ (s) | $T_{So}$ (s) | $T_{WB}$ (s) | $T_{Mo}$ (s) | $T_{RF.W}$ (s) | $T_{Ch\text{-}D,W}$ (s) |
|---|---|---|---|---|---|---|---|---|---|---|
| 1 | 297 | 132 | 111,954; 327,225[a];327,225[a]; 327,225[a] | 524,434 | 319,334 | 135,003 | 480,298 | 98,007 | 227,460 | 183,920 |
| 2 | 311 | 140 | 72,004; 114,601; 327,225[a]; 327,225[a] | 362,820 | 211,591 | 89,569 | 341,401 | 50,626 | 144,590 | 110,160 |
| 3 | 322 | 146 | 40,785; 54,150; 145,654; 76,037 | 284,934 | 168,104 | 70,098 | 264,164 | 44,785 | 103,513 | 76,791 |
| 4 | 338 | 153 | 27,933; 76,908; 32,918; 74,672 | 203,802 | 111,637 | 46,083 | 203,153 | 26,611 | 68,235 | 46,135 |
| 5 | 350 | 159 | 24,563; 34,586; 53,382; 29,875 | 170,070 | 96,060 | 38,294 | 164,210 | 26,611 | 51,066 | 34,827 |
| 6 | 361 | 165 | 18,846; 21,013; 28,584; 26,323 | 129,810 | 70,747 | 27,260 | 131,758 | 20,121 | 36,397 | 23,828 |
| 7 | 377 | 171 | 21,764; 9713; 28,116; 17,865 | 109,690 | 59713 | 22,717 | 108,392 | 20770 | 26,327 | 17,736 |
| 8 | 386 | 177 | 17,926; 18,035; 24,993; 10,279 | 85,675 | 44,784 | 16,226 | 88,920 | 16,875 | 24,116 | 12,388 |
| 9 | 398 | 186 | 13,905; 18,379; 5695; 8770 | 69,447 | 36,347 | 12,981 | 72,694 | 16,226 | 14,146 | 8978 |

[a] Specimen not subjected to failure.

sion-compression (load frequency 20 Hz) the following equation of the Wöhler curve was identified.

$$\log_{10}N_f = A - m \times \log_{10}\sigma_a = 29.69 - 9.8 \log_{10}\sigma_a \quad (18)$$

The fatigue limit is $\sigma_{af} = 252$ MPa which corresponds to $N_o = 1.25 \times 10^6$ cycles according (18) [1,2,4,19,21]. Specimens similar to those tested under constant amplitude loading were subjected to tests under random loading for tension-compression with the zero expected mean value and the parameters included into Table 1. The probability density function for the stress course $f(\sigma)$ (Fig. 3a) and the energy parameter $f(W)$ (Fig. 3b) are different. The distribution $f(\sigma)$ differs from the normal probability distribution (excess $< -1$, asymmetry $\approx 0$), while $f(W)$ takes similar values of excess and asymmetry as the normal probability distribution (excess $\approx 0$, asymmetry $\approx 0$).

Asymmetry is defined as

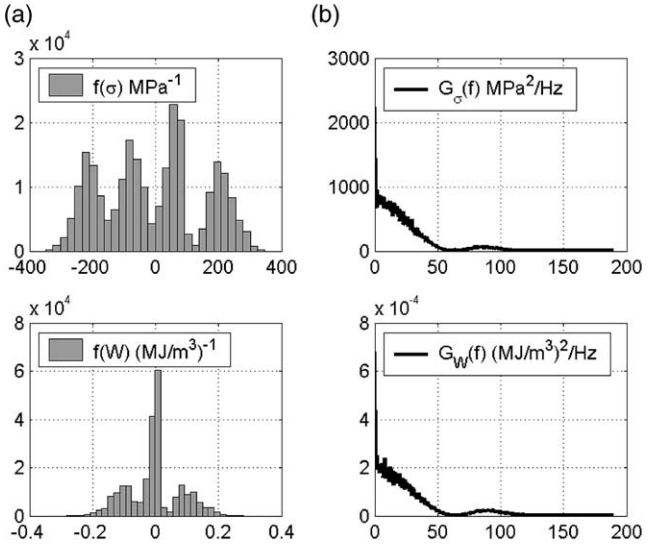


Fig. 3. (a) Probability density function for the courses $\sigma(t)$ and $W(t)$. (b) Power spectral density functions for $\sigma(t)$ and $W(t)$.

$$q_1 = \frac{\mu_3}{\mu_2^{3/2}} \quad (19)$$

and excess is defined as

$$q_2 = \frac{\mu_4}{\mu_2^2} - 3 \quad (20)$$

where $\mu_k$ is central moment of signal $x$, which is calculated by

$$\mu_k = E[(x - \hat{x})^k]. \quad (21)$$

Thus, we can draw a conclusion that in this case the energy parameter is a more suitable parameter to characterize the loading for spectral methods (Appendix 6), which assumes the normal probability distribution of a loading history [4].

For this steel, the FS parameter $k_1$ is 2.2, the material constant $k_2$ is 0.79 and the WB parameter $S$ is 1.44. For the Morel model the following parameters were identified: $p$ = 80,000 cycles, $q$ = 10,000 cycles and $r$ = 0 MPa·cycles [22].

## 10. Comparison between calculated and experimental fatigue lives

The fatigue test data for 36 specimens were compared with the calculation results. Figs. 4 and 5 show the points corresponding to the fatigue lives $T_{RF,W}$, $T_{CH\text{-}D,W}$ and the experimental ones $T_{exp}$. Observation time for the stress was $T_o$ = 649 s, and the sampling time was $\Delta t = 2.64 \times 10^{-3}$ s. The lives $T_{RF,W}$ can be accepted because they are included into the scatter band with coefficient 3 [17,19,21] in relation to the experimental lives $T_{exp}$, as in the case of tests under the constant amplitudes. The lives calculated with the spectral methods are satisfactory for the Chaudhury–Dover model ($T_{Ch\text{-}D,W}$).

From Table 1 and Figs. 4 and 5 it appears that the proposed approach to fatigue life determination seems

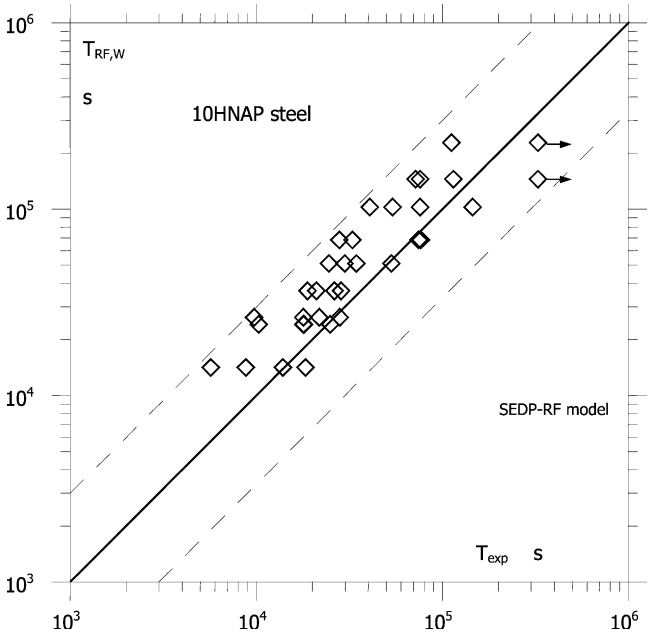


Fig. 4. Comparison of calculated life, $T_{RF,W}$ according to cycle counting from strain energy density parameter (SEDP) history with experimental life $T_{exp}$ under non-Gaussian random loading.

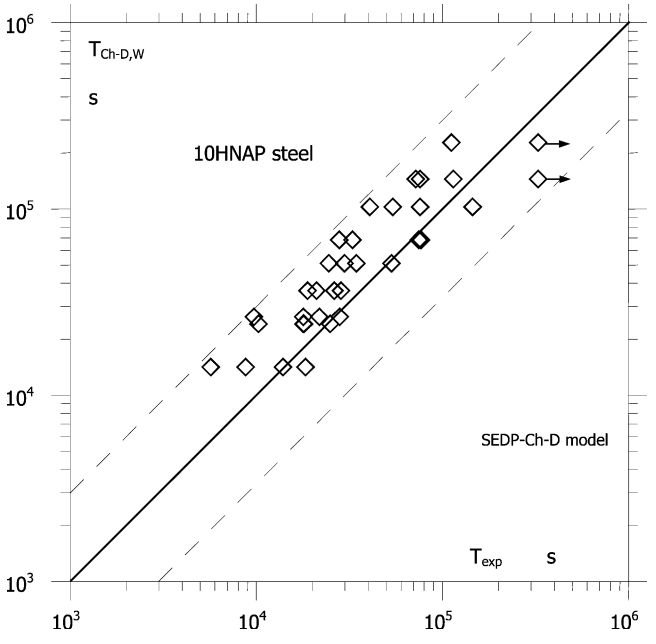


Fig. 5. Comparison of calculated life, $T_{Ch\text{-}D,W}$ according to the Choudhury–Dover model of spectral method and strain energy density parameter (SEDP) with experimental life $T_{exp}$ under non-Gaussian random loading.

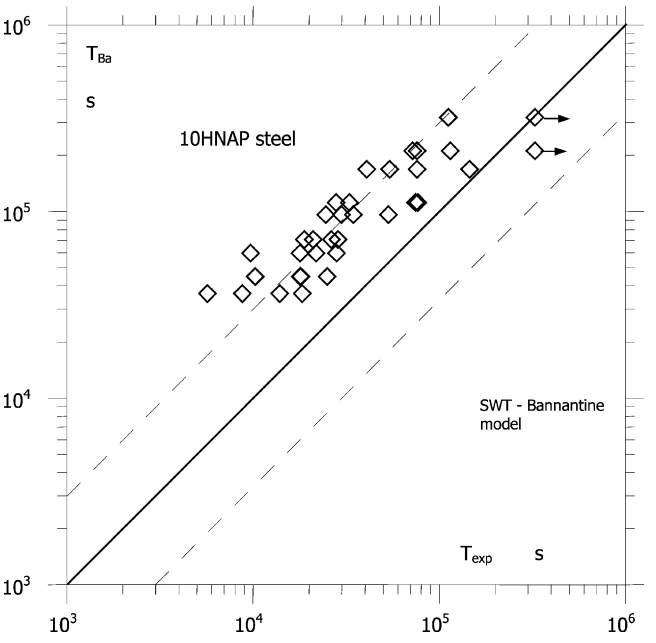


Fig. 6. Comparison of calculation life, $T_{Ba}$ according to the SWT parameter used by the Bannantine model with experimental life, $T_{exp}$ under non-Gaussian random loading.

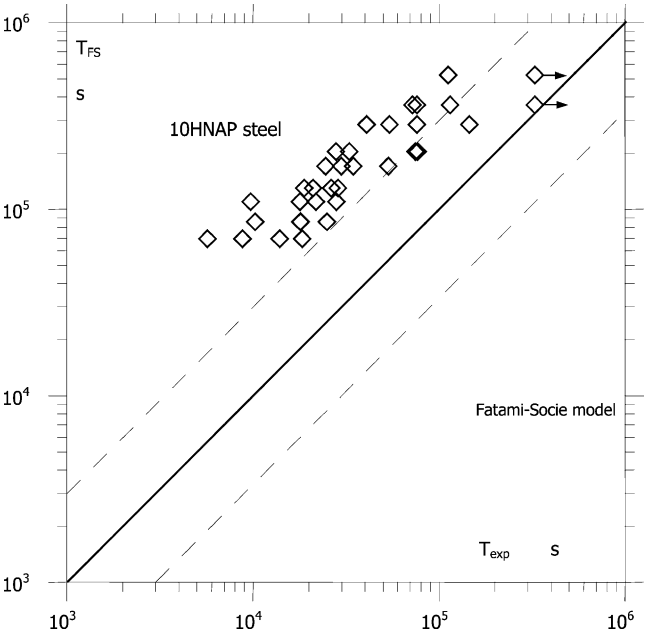


Fig. 7. Comparison of calculation life, $T_{FS}$ according to the Fatemi–Socie model with experimental life, $T_{exp}$ under non-Gaussian random loading.

to be very eff cient. Both the algorithmic method and the Chaudhury–Dover formula based on the strain energy density parameter give satisfactory results. We can expect that the proposed parameter is also eff cient for fatigue life determination under complex loading states. From Figs. 4 and 6–10 it appears that the best results are obtained for the strain energy density parameter and the Socie model. Some results obtained using the Morel model are out of the factor of 3 scatter band. For Bannantine, Wang–Brown and Fatemi–Socie models the calculated life times are too large. After analysing of six presented model it is possible to see that there are necessary to know some fatigue constants: for Fatemi–Socie 6; for Wang–Brown 8; SWT model and Morel 5, Socie

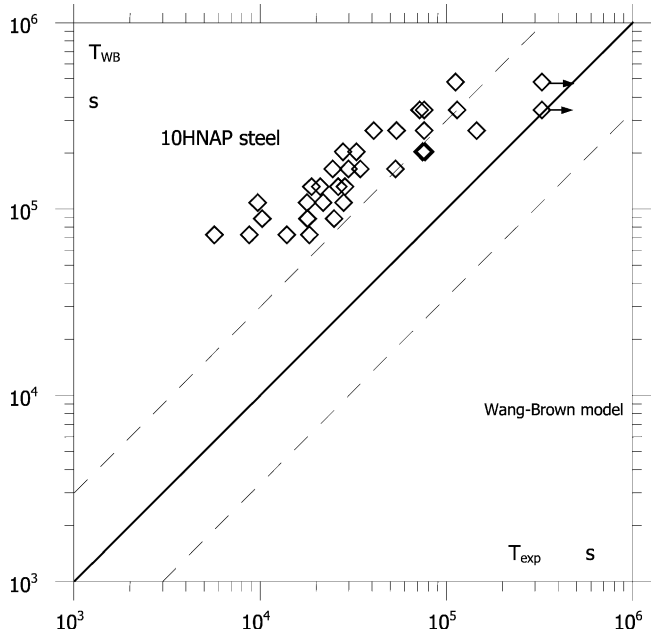


Fig. 8. Comparison of calculation life, $T_{WB}$ according to the Wang–Brown model with experimental life, $T_{exp}$ under non-Gaussian random loading.

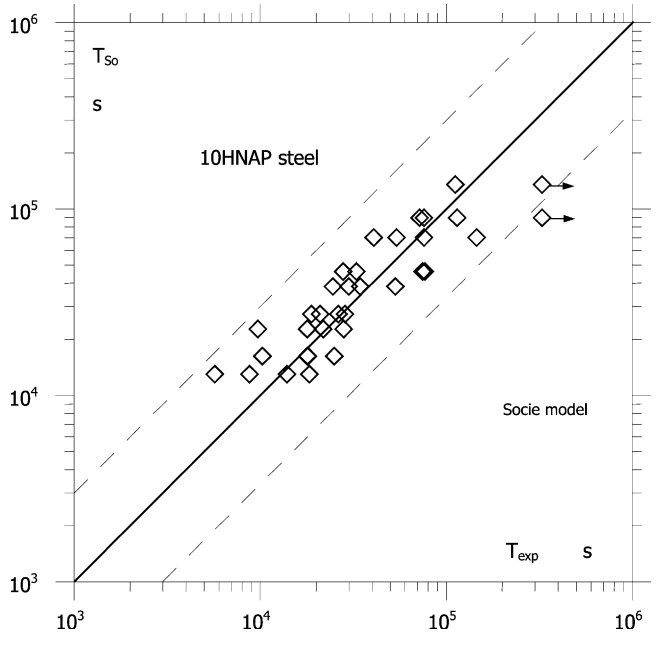


Fig. 9. Comparison of calculation life, $T_{So}$ according to the Socie model with experimental life, $T_{exp}$ under non-Gaussian random loading.

3 and for strain energy density parameter 3—practical 2 because the fatigue limit is not very important in this model.

For Fatemie and Socie's model, the Wang and Brown's and for the Socie's approach, the cycle counting parameter is computed on a critical plane related to axis ($x'$,$y'$,$n$) linked with this plane orientated by the unit

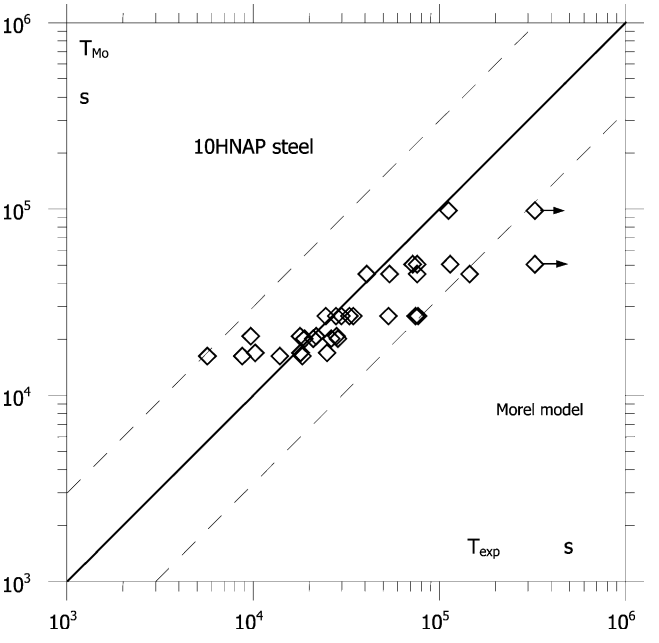


Fig. 10. Comparison of calculation life, $T_{Mo}$ according to the Morel model with experimental life, $T_{exp}$ under non-Gaussian random loading.

normal vector $\vec{n}$. Since $x'$ and $y'$ are arbitrary it is possible, especially under non-proportional loadings, that $x'$ and $y'$ do not coincide with the directions of the highest shear strain (or shear stress depending on the method). This means that, under non proportional loading, some damaging cycles can be omitted by the cycle counting procedure which does not count on the damage parameter but on an other variable. But in our push–pull tests this is not the case (proportional loadings). Nevertheless, the computation time for these models is short compare with the Morel approach. Other tests under non-proportional loadings have to be carried out to discuss this point in details with experimental data as reference in high cycle multiaxial fatigue.

## 11. Conclusions

Basing on the fatigue tests in high cycle regime of 10HNAP steel under uniaxial random stresses with non-Gaussian probability distribution function, zero mean value and wide-band frequency spectrum the following conclusions can be drawn:

1. The best and very similar results of fatigue life assessment has been obtained using strain energy density parameter both in time domain, $T_{RF,W}$, on the basis of the rainf ow algorithm and on frequency domain, $T_{Ch-D,W}$, on the basis of spectral method with Choudhury–Dover model.
2. The shear and normal stresses on the maximum shear stress plane model proposed by Socie gives also satis-

factory results included in a scatter band of the factor of 3 as for constant amplitude cyclic tests. Some results obtained using the Morel model are out of this scatter band

3. For Bannantine, Wang–Brown, Fatemi–Socie models calculated life times are not conservative.
4. It is also interesting to note, that for our experimental fatigue test data, the best predictions are obtained with the fatigue life calculation models for which the parameters have been identif ed on the elastic S–N curve (in Łagoda–Macha and Socie models). Furthermore, the high interest of the frequency domain approaches is the short computation time compared with the model in the time domain.


## Acknowledgements

With the support of the Commission of the European Communities under the FP5, GROWTH Programme, contract No. G1MA-CT-2002-04058 (CESTI).


## Appendix 1. : Algorithm used to apply the Fatemi-Socie model

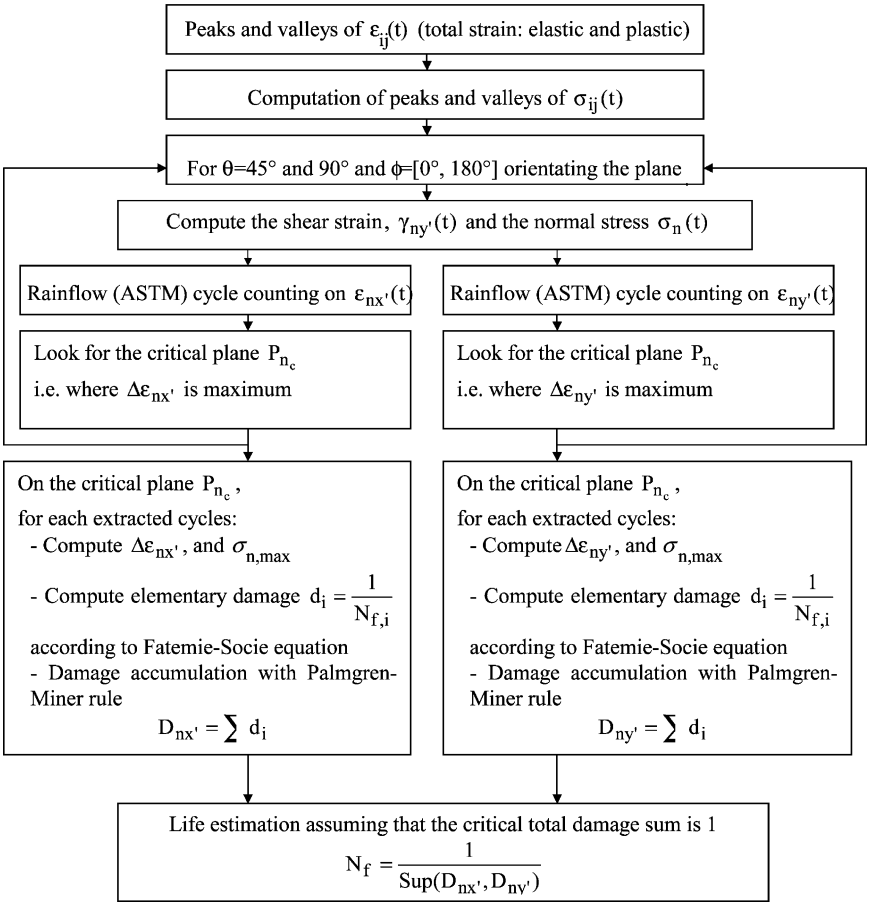

**Appendix 2. : Algorithm used to apply the Bannantine-Socie model with the SWT damage parameter**

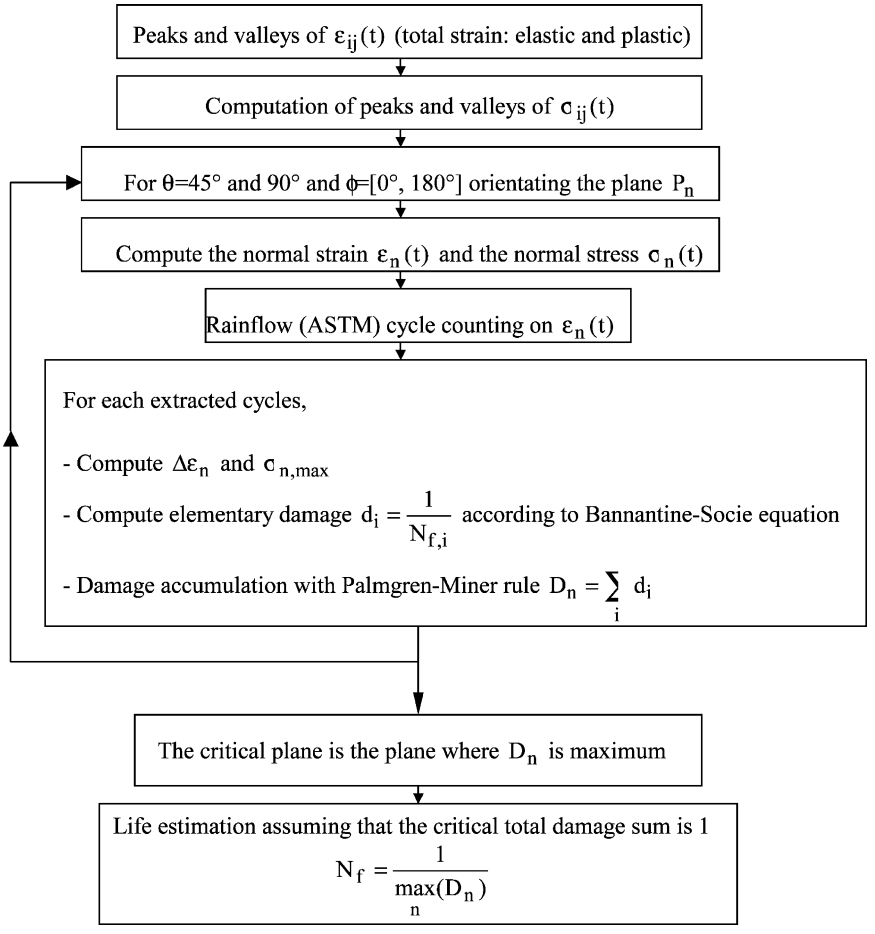

## Appendix 3. : Algorithm used to apply the Socie model in HCF

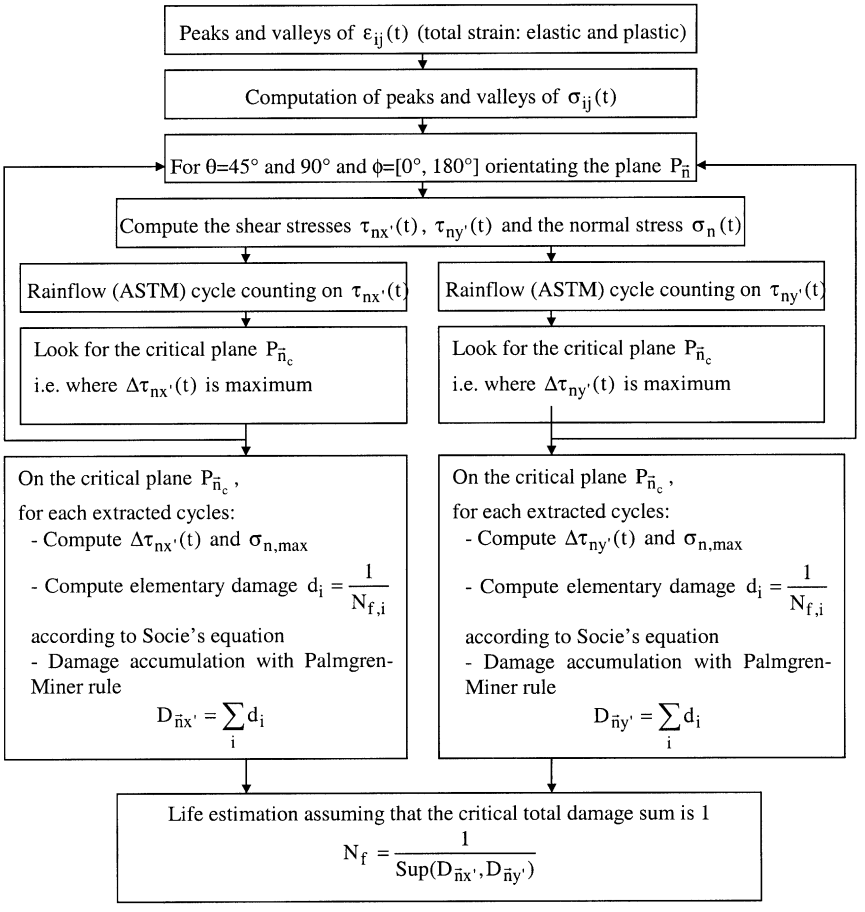

## Appendix 4. : Algorithm used to apply the Wang-Brown model

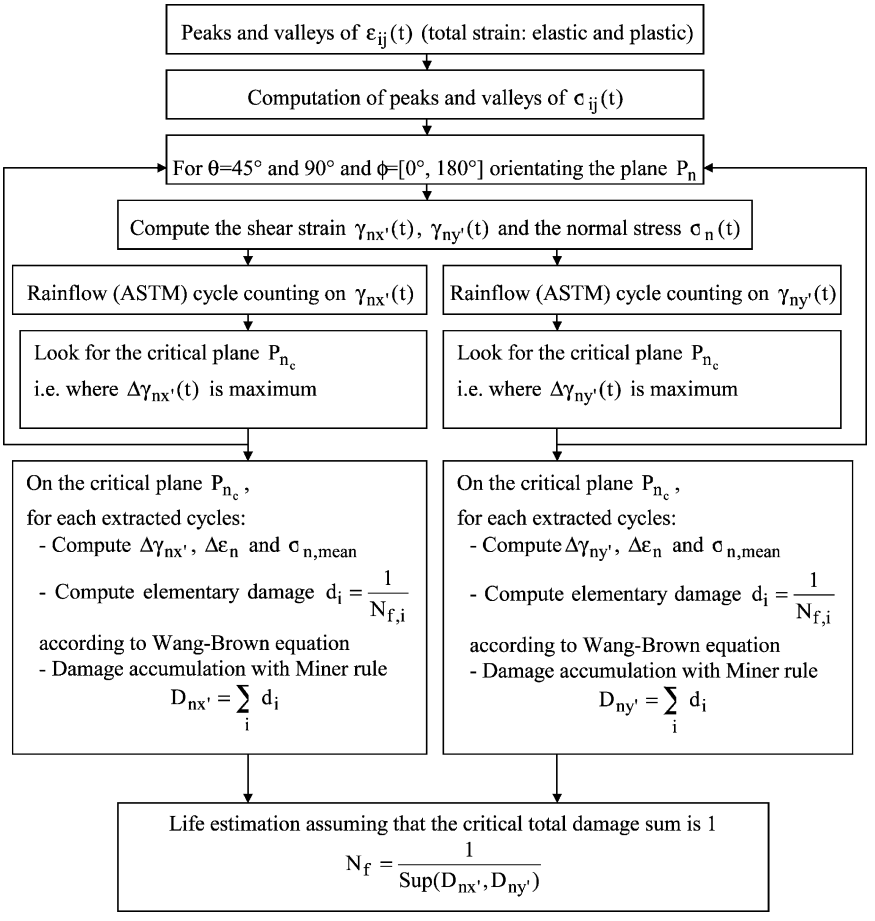

## Appendix 5. : Algorithm used to apply the Morel fatigue life calculation method

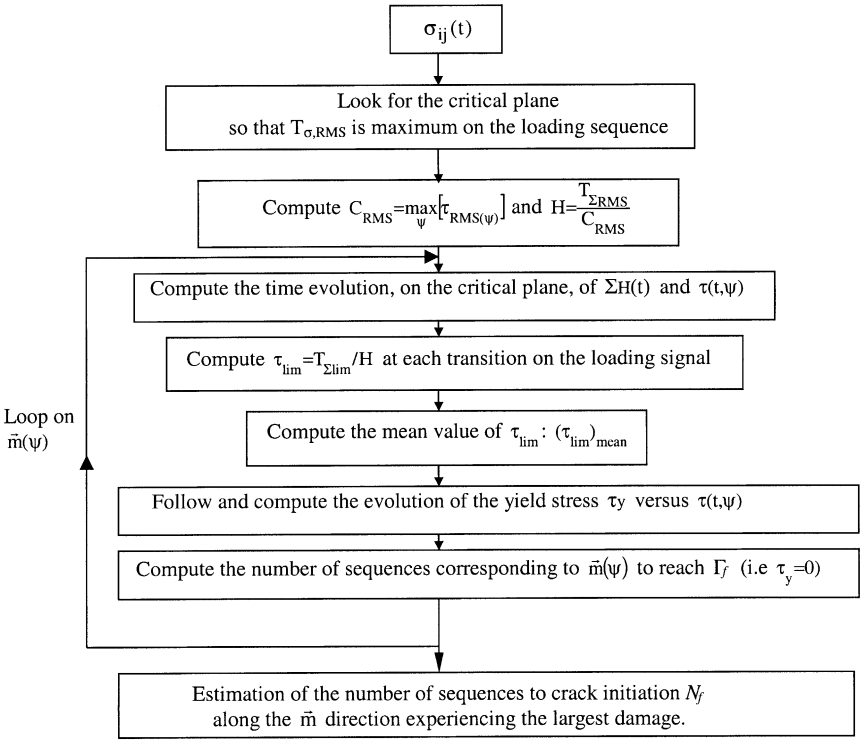


## Appendix 6. : Scheme showing differences and similarities between the calculation algorithms applied to fatigue life determination both in time and frequency domain

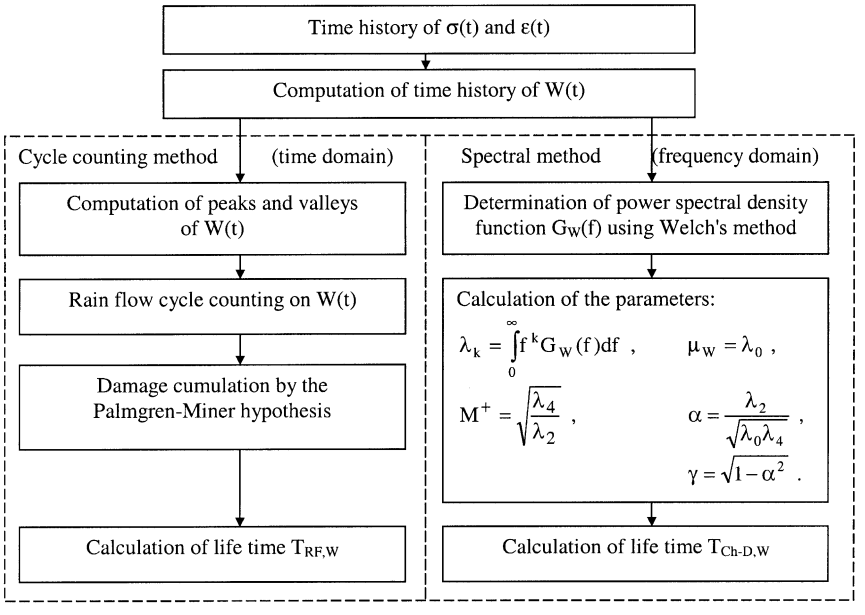

## References


[1] Łagoda T, Macha E. Generalization of energy multiaxial cyclic fatigue criteria to random loadings. In: Kalluri S, Bonacuse PJ, editors. Multiaxial fatigue and deformation: testing and prediction, ASTM STP 1387. West Conshohocken, PA: American Society for Testing and Materials; 2000. p. 173–90.

[2] Łagoda T, Macha E, Będkowski W. A critical plane approach based on energy concepts: Application to biaxial random tension-compression high-cycle fatigue regime. Int J Fatigue 1999;21(5):431–43.

[3] Łagoda T. Energy models for fatigue life estimation under random loading—part I—the model elaboration. Int J Fatigue 2001;23(6):467–80.

[4] Łagoda T. Energy models for fatigue life estimation under random loading—part II—verif cation of the model. Int J Fatigue 2001;23(6):481–9.

[5] Bannantine JA, Socie D. A variable amplitude multiaxial fatigue life prediction method. In: Kussmaul K, McDiarmid D, Socie D, editors. Fatigue under biaxial and multiaxial loading, ESIS 10. London: MEP; 1991. p. 35–51.

[6] Fatemi A, Socie DF. A critical plane approach to multiaxial fatigue damage including out-of-phase loading. Fatigue Fract Engng Mater Struct 1988;11(3):149–65.

[7] Socie D. Critical plane approaches for multiaxial fatigue damage assessment. In: McDowell DL, Ellis R, editors. Advances in multiaxial fatigue, ASTM STP 1191. Philadelphia, PA: ASTM; 1993. p. 7–36.

[8] Wang CH, Brown MW. A path-independent parameter for fatigue under proportional and non-proportional loading. Fatigue Fract Engng Mater Struct 1993;16(12):1285–98.

[9] Wang CH, Brown MW. Multiaxial random load fatigue: life prediction techniques and experiments. In: Pineau A, Cailletaud G, Lindley TC, editors. Multiaxial fatigue and design, ESIS 21. London: MEP; 1996. p. 513–27.

[10] Morel F. A critical plane approach for life prediction of high cycle fatigue under multiaxial variable amplitude loading. Int J Fatigue 2000;22:101–19.

[11] Morel F. Fatigue multiaxiale sous chargement d'amplitude variable. PhD thesis, University of Poitiers, France, 1996.

[12] Morel F. A fatigue life prediction method based on a mesoscopic approach in constant amplitude multiaxial loading. Fatigue Fract Engng Mater Struct 1998;21:241–56.

[13] ASTM Standard practices for cycle fatigue counting in fatigue analysis, Designation E 1049-85, vol. 03.01 of metal test methods and analytical procedure. Philadelphia, PA: ASTM; 1985. p. 836–48.

[14] Bannantine JA, Socie DF. Multiaxial fatigue life estimation techniques. In: Mitchell M, Landgraf R, editors. Advances in fatigue lifetime prediction techniques, ASTM STP 1122. Philadelphia, PA: ASTM; 1992. p. 249–75.

[15] Sonsino CM, Kaufman H, Grubisic V. Transferability of material data for the example of a randomly loaded truck stub axle, SAE Tech. paper series, 970708, 1997. p. 1–22.

[16] Fatemi A, Kurath P. Multiaxial fatigue life predictions under the inf uence of mean-stresses. J Engng Mater Tech Trans ASME 1988;110:380–8.

[17] Chaudhury GK, Dover WD. Fatigue analysis of offshore platforms subject to sea wave loadings. Int J Fatigue 1985;7(1):13–9.

[18] Liu HJ, Hu SR. Fatigue under non normal random stresses using Monte - Carlo method. In: Ritchie RO, Starke Jr EA, editors. FATIGUE '87. EMAS; 1987. p. 143–9.

[19] Lachowicz C, Łagoda T, Macha E. Comparison of analytical and algorithmical methods for life time estimation of 10HNAP steel under random loadings, In: Lutjering G, Nowack H, editors. Fatigue 96, vol. I, Berlin, 1996. p. 595–600.

[20] MSC/FATIGUE user's guide, vibration fatigue theory, pp. 644–8.

[21] Lachowicz C, Łagoda T, Macha E, Dragon A, Petit J. Selections of algorithms for fatigue life calculation of elements made of 10HNAP steel under uniaxial random loadings. Studia Geotechnika et Mechanica 1996;XVIII(1-2):19–43.

[22] Banvillet A. Prévision de durée de vie en fatigue multiaxiale sous chargements reels: vers des essais accéléres. PhD thesis, ENSAM, Centre de Bordeaux, 2001. p. 201.